

Optical characterization of salt-induced swelling behavior of poly(*N*-isopropylacrylamide) terpolymer hydrogel layers

İlke ANAÇ^{1,*} , Anıl BOZDOĞAN^{1,2} ¹Department of Materials Science and Engineering, Gebze Technical University, Gebze, Kocaeli, Turkey²Health and Environment Department, AIT-Austrian Institute of Technology GmbH, Vienna, Austria

Received: 06.03.2019

Accepted/Published Online: 08.05.2019

Final Version: 06.08.2019

Abstract: This study reports for the first time the effect of different sodium halide salts (NaClO_4 , NaI , and Na_2CO_3) in the low concentration range (in the range of 10^{-7} – 1 M) on the swelling behavior of photo-crosslinked, surface-immobilized poly(*N*-isopropyl acrylamide) (PNIPAAm) terpolymer layers. PNIPAAm terpolymer (consisting of *N*-isopropylacrylamide, methacrylic acid, and 4-methacryloxybenzophenone) was synthesized via free radical polymerization. The PNIPAAm terpolymer layers were prepared on gold substrates via spin coating and crosslinked and surface attached via UV radiation. The swelling behavior of the layers in monovalent (NaClO_4 and NaI) and divalent (Na_2CO_3) solutions was monitored by surface plasmon/optical waveguide spectroscopy. The terpolymer layers did not swell significantly at very low salt concentrations (10^{-7} – 10^{-5} M), whereas an increase in swelling upon the addition of salt up to 10^{-2} – 0.1 M depending on the salt was observed. Further increase in the salt concentration up to 1 M led to collapse of the terpolymer PNIPAAm layers due to the reduction in solvent quality of the salt solution. The full collapse of the terpolymer PNIPAAm layers with 1 M salt solution was observed only when divalent kosmotropic Na_2CO_3 salt was used.

Key words: Salt effect, poly(*N*-isopropylacrylamide), surface plasmon resonance spectroscopy, stimulus-responsive hydrogel

1. Introduction

Stimulus-responsive hydrogels, or “smart” hydrogels, are crosslinked, water-swollen polymer networks that alter their water content by undergoing significant swelling and contraction in response to changes in surrounding aqueous medium such as temperature [1,2], pH [3,4], ionic strength [5], pressure [6], and magnetic [7] and electric fields [8]. Owing to this responsive behavior, these materials can be used in many fields such as drug delivery systems [9,10], separation materials [11], actuators [12], sensors [13], and chromatographic support [14]. The swelling behavior of surface-attached hydrogel layers is quite anisotropic compared to the bulk hydrogels as the swelling is only allowed in the direction perpendicular to the substrate while being forbidden in the lateral direction [15–17]. This reduces the swelling degree and hinders the full collapse of hydrogels. Changes in the lower critical solution temperature of stimulus-responsive hydrogels are also observed due to the constraints when immobilized on solid substrates in the literature [2,6,18–20].

The effects of temperature, pH, crosslinking density, and ionizable groups on the swelling behavior of surface-attached *N*-isopropylacrylamide (NIPAAm)-based hydrogel layers were studied in detail by different

*Correspondence: ilkeanac@gtu.edu.tr

research groups using ellipsometry [20,21], surface plasmon resonance spectroscopy (SPR) [6,17–19,22], neutron reflection [23], and atomic force microscopy (AFM) [23,24] in the literature. The local and global dynamic properties of swollen poly(*N*-isopropyl acrylamide) (PNIPAAm) gels immobilized on solid surfaces were characterized using fluorescence correlation spectroscopy (FCS) [25] and dynamic micro light scattering [26,27]. Harmon et al. studied the effect of pH and temperature on the swelling of *N*-isopropylacrylamide-based copolymer and terpolymer thin layers [18,19]. They found that the volume phase transition temperature changes between 25.3 and 44.9 °C for 200 nm films depending on the pH of the solution. They also found that the swelling behavior of the hydrogel layers changes as a function of dry film thickness [18,19]. Beines et al. studied the temperature-induced volume phase transition of NIPAAm-based terpolymer thin layers containing methacrylic acid and sodium methacrylate [22]. Refractive index gradient, which was not present in free acid gels, was found in the swollen hydrogel films containing sodium methacrylate [22]. Neutron reflectivity studies of the photo-crosslinked PNIPAAm layers by Vidyasagar et al. showed that water is expelled discontinuously at low crosslink densities but continuously at high crosslink densities [23].

Besides temperature and pH, the salt-induced swelling behavior of PNIPAAm brushes and thin gel films was studied by several research groups [17,22,28–33]. Ishida et al. studied the Na_2SO_4 salt-induced changes in grafted PNIPAAm layers using quartz crystal microbalance (QCM-D) with dissipation and AFM and used high salt concentrations in the range of 0.1 to 1 M [29]. They found that the critical concentration for brush collapse was at 0.11 M salt concentration where a significant change in the frequency dissipation data obtained by QCM-D was seen [29].

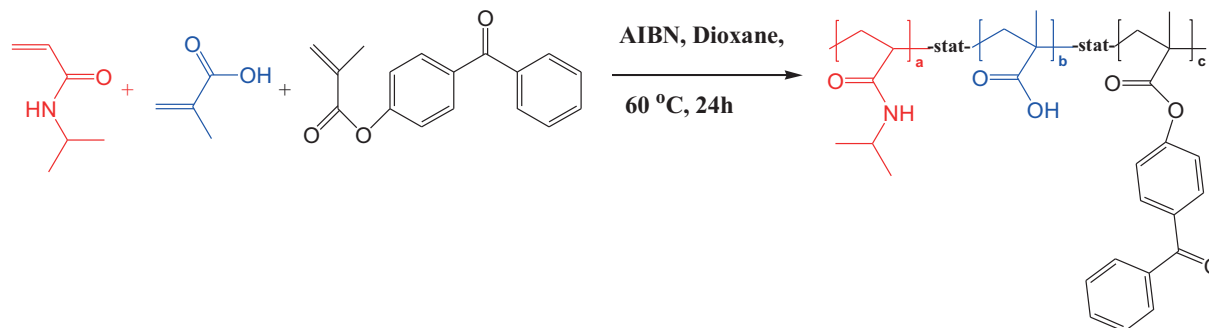
Naini et al. studied the effect of different sodium halides (NaI, NaBr, and NaCl) at 0.25 M on the temperature-dependent behavior of PNIPAAm brushes using the laser temperature-jump technique and found that the transition temperature was affected according to the halides' order in the Hofmeister series [30]. The effect of specific anions (SCN^- and CH_3CO_2^-) on the equilibrium thermoresponse of PNIPAAm brushes was studied using in situ ellipsometry, quartz crystal QCM-D, static contact angle measurements, neutron reflectometry (NR), and AFM [31,32]. It was found that the shift in transition temperature was in line with the Hofmeister series where transition temperature was shifted to lower temperature by kosmotropic acetate ions and higher temperature by chaotropic thiocyanate ions [31,32]. Koenig et al. studied the effect of NaCl salt on the thermoresponsive behavior of PNIPAAm brushes using QCM and ellipsometry and found that transition temperature was shifted to lower temperatures by the addition of NaCl salt due to the interaction of the ions with the amide groups and the hindrance of hydrogen-bonding formation [33]. The concentration of salts used in all the studies was in the range of 0.01–5 M. To the best of our knowledge, there are only two studies that examined the effect of very low salt concentration (in the range of 10^{-7} –1 M) on the swelling behavior of PNIPAAm thin layers. In these studies NaCl was used as a salt and its effect on the swelling behavior was characterized via SPR [17,28] and light micro-photon correlation spectroscopy (μPCS) [28]. It was found that the thickness of PNIPAAm layers increases at intermediate NaCl concentrations and then decreases as the NaCl concentration increases [17,28].

To date, as explained above, the salt-induced swelling behavior of PNIPAAm thin layers in the very low concentration range (in the range of 10^{-7} –1 M) was only studied using NaCl salt [17,28]. The effect of different sodium halide salts in the Hofmeister series in the very low concentration range was not studied before in the literature. In order to fill this gap in the literature, the salt-induced swelling behavior of photo-crosslinked PNIPAAm terpolymer thin films in different sodium halides (NAI, NaClO_4 , and Na_2CO_3) in the

concentration range from 10^{-7} to 1 M was investigated using SPR/optical waveguide spectroscopy (OWS) in the present study. The stimulus-responsive terpolymer used in this study consists of NIPAAm, methacrylic acid (MAA), and 4-methacryloxybenzophenone (MABP). NIPAAm gives the responsive character. MAA as an ionic monomer prevents the “skin barrier” [34] (thin, dense outer layer), which forms during collapse and slows down the gel collapse. The MABP was incorporated in the polymer backbone as a crosslinking unit. The thin terpolymer layer was prepared on benzophenone functionalized gold surfaces via spin coating and crosslinked and surface attached via UV irradiation through benzophenone groups on the gold surfaces and polymer backbone.

2. Results and discussion

In the present study, the effect of different salt solutions (NaClO_4 , NaI, and Na_2CO_3) on the swelling behavior of photo-crosslinked PNIPAAm terpolymer layers was studied using SPR/OWS spectroscopy. PNIPAAm terpolymer (containing 94% NIPAAm, 5% MAA, and 1% MABP) was synthesized by free radical polymerization in anhydrous dioxane using AIBN as an initiator (Scheme). The crosslinked PNIPAAm terpolymer thin films ($d_{dry} \sim 1 \mu\text{m}$) were prepared via spin coating from a PNIPAAm terpolymer solution onto propyl-3-(4-benzoylphenoxy) thioacetate (BPSAc)-modified SPR substrates in ethanol and via UV irradiation at 365 nm for 1 h, respectively. Crosslinking of the PNIPAAm terpolymer layers and attachment of the terpolymer layer to the modified SPR substrates via UV radiation were achieved through MABP groups [35].



Scheme. Synthesis of PNIPAAm statistical (stat) terpolymer [27].

Figures 1a–1c show the SPR/OWS raw data and corresponding fits based on a “box model” of PNIPAAm terpolymer thin layers in the dry state, in water, and in 10^{-6} M NaClO_4 solution, respectively. As seen from Figure 1a, the SPR/OWS spectrum of the dry film shows a broad minimum around 78.1° (surface plasmon mode (TM₀)) and four waveguide modes (TM₁–TM₄ from right to left). A box model [26], which takes an average refractive index for the film, was used to fit the SPR/OWS data and the thickness and the refractive index of the PNIPAAm layers were calculated. The refractive index and the thickness of the dry PNIPAAm layer were 1.48 and $1.17 \mu\text{m}$, respectively. The surface plasmon mode (TM₀) shifts to lower angle (62.08° (water) and 62.31° (NaClO_4)) and waveguide modes (TM₁–TM₄) are placed closer to each other due to the swelling of the PNIPAAm layer in water and in 10^{-6} M NaClO_4 solution (Figures 1b and 1c). The thickness of PNIPAAm layers swollen in water and in 10^{-6} M NaClO_4 solution was $3.88 \pm 0.05 \mu\text{m}$ and $3.55 \pm 0.05 \mu\text{m}$, respectively.

Figures 2a and 2b and 3a and 3b show the measured SPR/OWS data of PNIPAAm layers in contact with

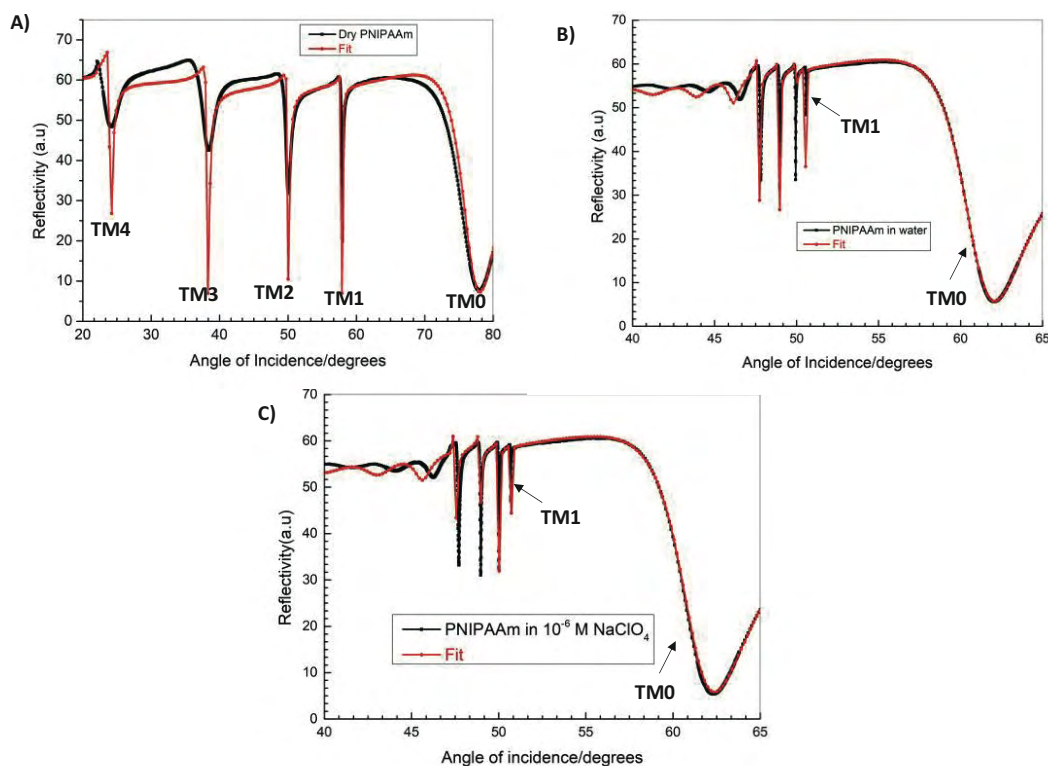


Figure 1. SPR/OWS spectrum of PNIPAAm terpolymer thin films crosslinked via UV radiation (365 nm) for 1 h (a) in the dry state ($d_{dry} = 1.17 \mu\text{m}$), (b) swollen in water at room temperature ($d_{water} = 3.82 \mu\text{m}$), and (c) in 10^{-6} M NaClO_4 ($d_{\text{NaClO}_4} = 3.56 \mu\text{m}$). Black lines are the measured spectra and red lines are the fit based on the “box model”.

NaClO_4 solution and NAI solution having concentration in the range of 10^{-7} to 1 M, respectively. An increase in the number of waveguide modes was observed in 10^{-3} M and 10^{-4} M NAI solutions and this can only be explained by enormous swelling of PNIPAAm layers at these concentrations (Figures 3a and 3b), whereas no increase in waveguide modes in NaClO_4 solution was seen at any concentration. The shifts in surface plasmon minimum (TM0) and TM1 modes as a function of salt concentration were observed in both salt solutions. The graph in Figure 4a also shows surface minimum angle and coupling angles from TM1 mode as a function of NaClO_4 and NAI concentration in the range of 10^{-7} to 1 M. In both salt solutions, there was almost no change in TM0 and TM1 angles up to 10^{-5} M salt concentration. A decrease in TM0 and TM1 angles was observed with an increase in salt concentration up to 0.1 M due to the swelling of PNIPAAm layers. In both salt solutions, 0.1 M is the limiting value because an increase in TM0 and TM1 angles was observed with a further addition of salt. The PNIPAAm layer collapses as the salt concentration exceeds 0.1 M for both salts.

The thickness and refractive index values calculated using a “box model” as a function of NaClO_4 concentration are depicted in Figure 4b. There was a slight decrease in thickness values and a slight increase in refractive index values up to 10^{-5} M, indicating that the PNIPAAm layer slightly collapses as the NaClO_4 concentration increases from 10^{-7} M ($3.66 \pm 0.05 \mu\text{m}$) to 10^{-5} M ($3.55 \pm 0.05 \mu\text{m}$). The thickness values increased from $3.55 \pm 0.05 \mu\text{m}$ to $4.83 \pm 0.05 \mu\text{m}$ and the refractive index values decreased from 1.374 to 1.369 as the salt concentration rose from 10^{-5} M to 10^{-2} M. This shows that the PNIPAAm layer clearly swelled and the layer thickness reached a global maximum value at a salt concentration of 10^{-2} M. The collapse of the

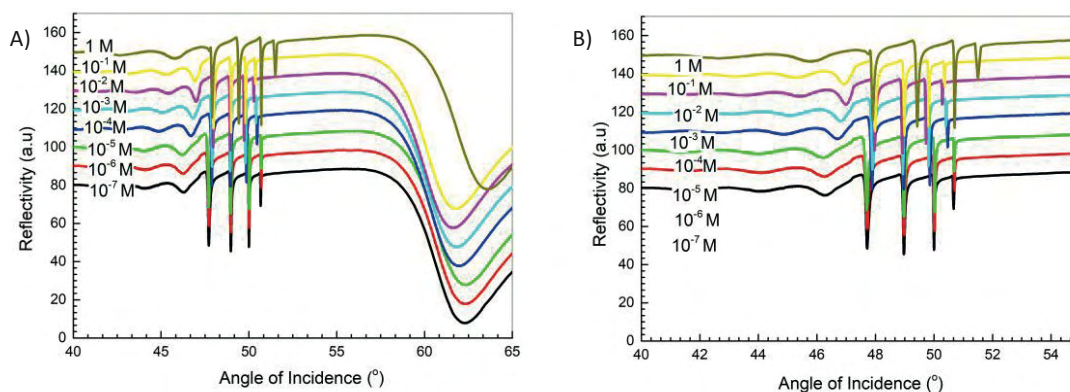


Figure 2. (a) SPR/OWS spectra and (b) magnification of optical waveguide mode regions of PNIPAAm terpolymer thin films crosslinked via UV radiation (365 nm) for 1 h in 10^{-7} –1 M NaClO_4 solutions.

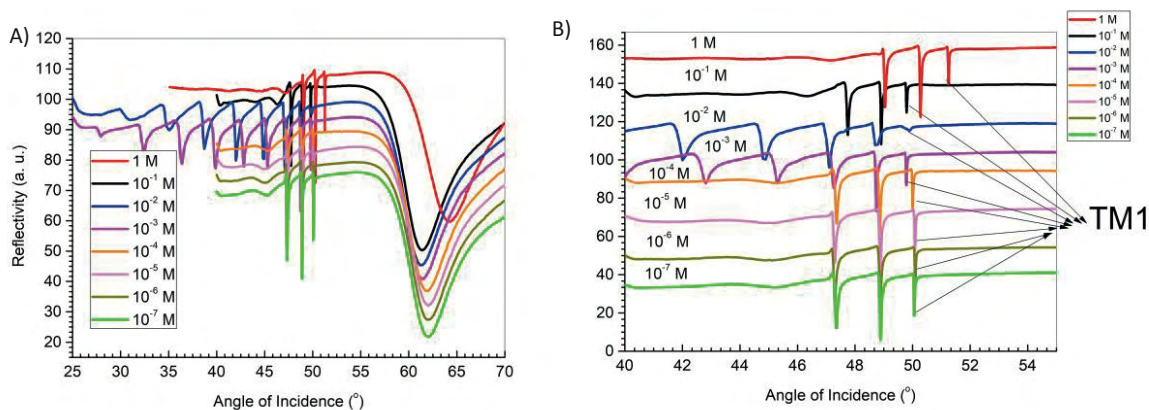


Figure 3. SPR/OWS spectra (a) and magnification of optical waveguide mode regions (b) of PNIPAAm terpolymer thin films crosslinked via UV radiation (365 nm) for 1 h in 10^{-7} –1 M NaI solutions.

PNIPAAm layer started with the addition of NaClO_4 beyond 10^{-2} M and the thickness of the layer decreased to $3.20 \mu\text{m}$ at 1 M. This is not totally consistent with the graph of TM0 and TM1 values vs. salt concentration (Figure 4a), where the highest swelling was obtained at 0.1 M salt concentration. The difference can be due to the thickness and refractive index calculation based on the “box model”, which assumes that the layer is homogeneous and takes an average refractive index value for the whole layer. As seen from Figure 1c, the fit is not perfect, showing that the refractive index is not uniform in the swollen layer. Figures 4a and 4b show that the PNIPAAm layer swells to a maximum value with the addition of a monovalent salt (NaClO_4 or NaI) up to 10^{-2} –0.1 M, and starts to collapse as the concentration of salt exceeds 10^{-2} –0.1 M. The results are consistent with the literature, where the same trend was observed for NaCl salt [17,28].

The salt-induced swelling behavior of the PNIPAAm layer at low monovalent NaClO_4 and NaI salt concentrations can be explained by an increase in osmotic pressure in the layer. This increase in the osmotic pressure is due to (a) proton exchange from the carboxylic acid group by counterions such as ClO_4^- or I^- and (b) diffusion of ions (Na^+ , ClO_4^- , and I^-) into the PNIPAAm layer. The maximum swelling of the layer (around 10^{-2} M–1 M in the present study) occurs when the salt concentration in the aqueous media outside PNIPAAm layer is equal to the free ions inside the layer. At high NaClO_4 and NaI salt concentrations, the

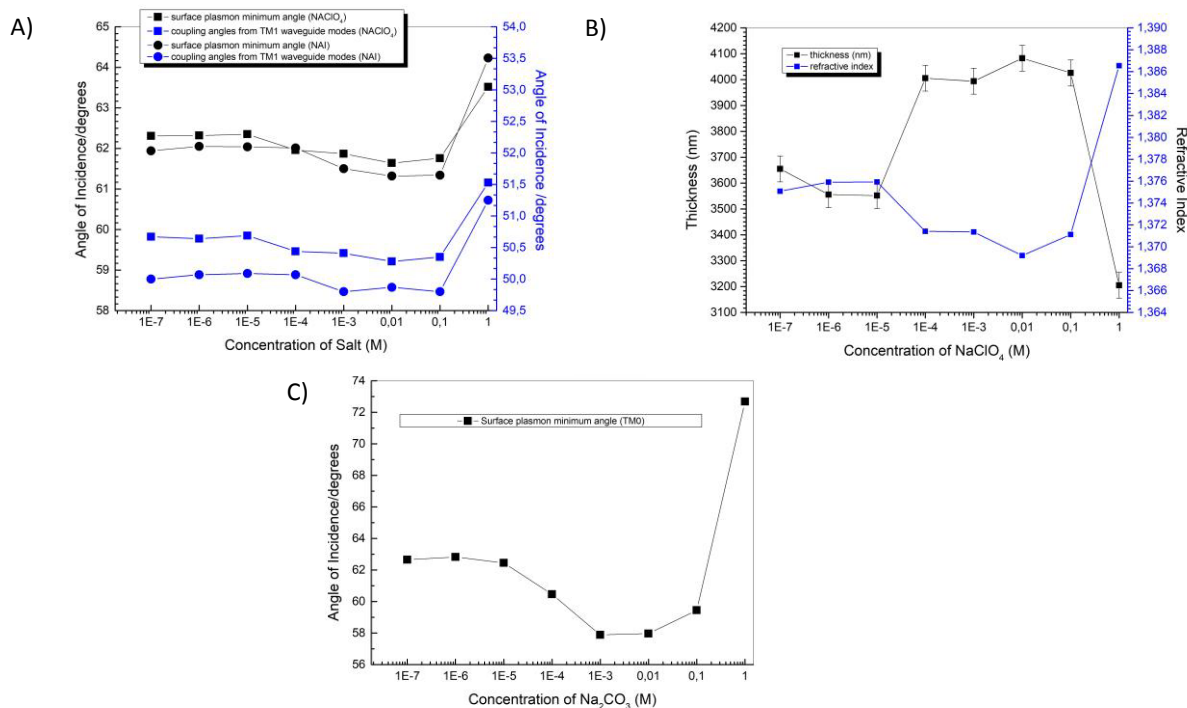


Figure 4. (a) Surface plasmon minimum angle (black) and coupling angles from TM1 waveguide modes (blue) of photo-crosslinked PNIPAAm terpolymer thin films versus NaClO₄ (square) and NaI (circles) concentration, (b) thickness and refractive index values of thin films obtained by fit based on the box model versus NaClO₄ salt concentration, (c) surface plasmon minimum angle of thin films versus Na₂CO₃ concentration.

drop in solvent quality accounts for the collapse of the PNIPAAm layer (salt-out effect). The drop in solvent quality can be explained by the screening of carboxylate groups by the addition of salt ions. Similar effects of NaCl salt for PNIPAAm layers [19,28] and polymethacrylic acid brushes [36] were also reported in the literature.

The effect of a divalent salt, Na₂CO₃, at low salt concentrations (10⁻⁷ – 1 M) on the swelling behavior of PNIPAAm layers was also studied by SPR/OWS spectroscopy. Figure 4c shows the surface plasmon minimum angle (TM0) as a function of Na₂CO₃ salt concentration. It was very hard to see the waveguide modes in Na₂CO₃ salt solution at all the concentrations due to the inhomogeneous layer structure and inefficient coupling of the waveguide modes and so only the surface plasmon minimum angle was plotted as a function of salt concentration. A decrease in TM0 angle was also seen as the Na₂CO₃ concentration increased from 10⁻⁷ M to 10⁻² M due to layer expansion. The layer started to collapse with further addition of Na₂CO₃ salt beyond 0.01 M. The surface plasmon minimum angle (TM0) was enhanced to 72.7°, which is very close to the TM0 angle (78.1°) of the PNIPAAm layer in the dry state, indicating the full collapse of the PNIPAAm layer at 1 M Na₂CO₃ solution. This can be explained by the strong solubility reduction ability of CO₃²⁻ anions, on the left in the Hofmeister series, at low concentrations compared to ClO₄⁻ or I⁻ anions.

Summarizing, in the present study, we examined the salt-induced volume phase transition of PNIPAAm layers in monovalent (NaClO₄ and NaI) and divalent (Na₂CO₃) salt solutions in a low concentration regime (10⁻⁷–1 M) for the first time using the SPR/OWS technique. At very low salt concentrations (10⁻⁷–10⁻⁵ M) the swelling of the layers did not change significantly, whereas a large increase in swelling was observed upon

the addition of salt up to 10^{-2} –0.1 M, depending on the salt due to the osmotic pressure increase inside the layer. A further increase in the salt concentration led to a reduction in the solvent quality of the salt solution and due to this PNIPAAm layers started to collapse at high salt concentrations (1 M). The PNIPAAm layers fully collapsed at 1 M salt solution when a divalent kosmotropic salt (Na_2CO_3) was used.

3. Experimental details

3.1. Materials

NIPAAm (99%), 2,2'-azo bis(2-methyl-propionitrile) (AIBN, 98%), MAA (99%), 1,4 dioxane (anhydrous, 99.8%), sodium iodide (NaI), sodium perchlorate (NaClO_4) ethanol, diethyl ether, and toluene were purchased from Aldrich. Sodium carbonate (Na_2CO_3) and hexane were purchased from Merck. The NaI, NaClO_4 , and Na_2CO_3 were used as received. The NIPAAm and AIBN were recrystallized from a toluene/hexane (1/4) mixture and methanol, respectively. MAA was purified by passing through a basic alumina column. Distilled water ($18.2 \text{ M}\Omega \text{ cm}^{-1}$) was purified by an Elga Option Q15 water purification system. MABP [20] and propyl-3-(4-benzoylphenoxy) thioacetate (BPSAc) [22] were synthesized as described in the literature. LASFN9 glass slides were obtained from Hellma Optik GmbH (Jena, Germany).

3.2. Synthesis of PNIPAAm terpolymer

NIPAAm-based terpolymer was synthesized by free radical polymerization of NIPAAm (94% monomer concentration), MAA (5% monomer concentration), and MABP (1% monomer concentration) according to the literature [16,22] (Scheme). The composition of the terpolymer was calculated as 86% NIPAAm, 5% MAA, and 9% MABP. The polymerization was conducted in anhydrous dioxane at 60°C under argon for 24 h and AIBN was used as an initiator. The polymer was precipitated via pouring the reaction mixture into cold diethyl ether, and the polymer was reprecipitated from methanol solution and filtered and dried under vacuum at 60°C overnight. The reaction yield was 73%.

^1H NMR (CCl_3D): δ/ppm : 0.67–1.20 (m, $-\text{CH}_3$), 1.20–1.74 (m $-\text{CH}_2-$), 1.74–2.40 (m, NIPAAm backbone, CH), 3.70 (s, $\text{CH}_3-\text{CH}-\text{CH}_3$), 7.40–8.20 (CH aromatic)

The molecular weight of the terpolymer was determined using gel permeation chromatography via a Waters 2414 refractive index detector and three Styragel columns (HT2, HT3, and HT4). The measurement was conducted in tetrahydrofuran (THF) at 30°C with a flow rate of 0.35 mL/min. The molecular weight (M_w) and the polydispersity index (M_w/M_n) were 102,279 g/mol and 2.26, respectively.

3.3. Preparation of PNIPAAm terpolymer thin films

LaSFN9 glass slides (25.4 mm P 25.4 \times 1.5 mm) were coated with chromium (2 nm) and gold (50 nm) using a Nanovak NVTE4-01 thermal evaporator. The coated glass slides were dipped in 0.005 M BPSAc ethanolic solution at room temperature overnight, and then washed with ethanol and dried under argon flow. PNIPAAm hydrogel thin layers were prepared by spin coating (5000 rpm, 1 min, Laurell WS-650-23 spin coater) from 8% w/v PNIPAAm terpolymer ethanol solution onto glass slides that were coated with BPSAc, and then dried in a vacuum oven at 50°C overnight. The hydrogel layer was crosslinked and attached to the BPSAc modified substrate via UV radiation (365 nm) for 1 h (Herolab CL-1 UV crosslinker) (Figure 5a).

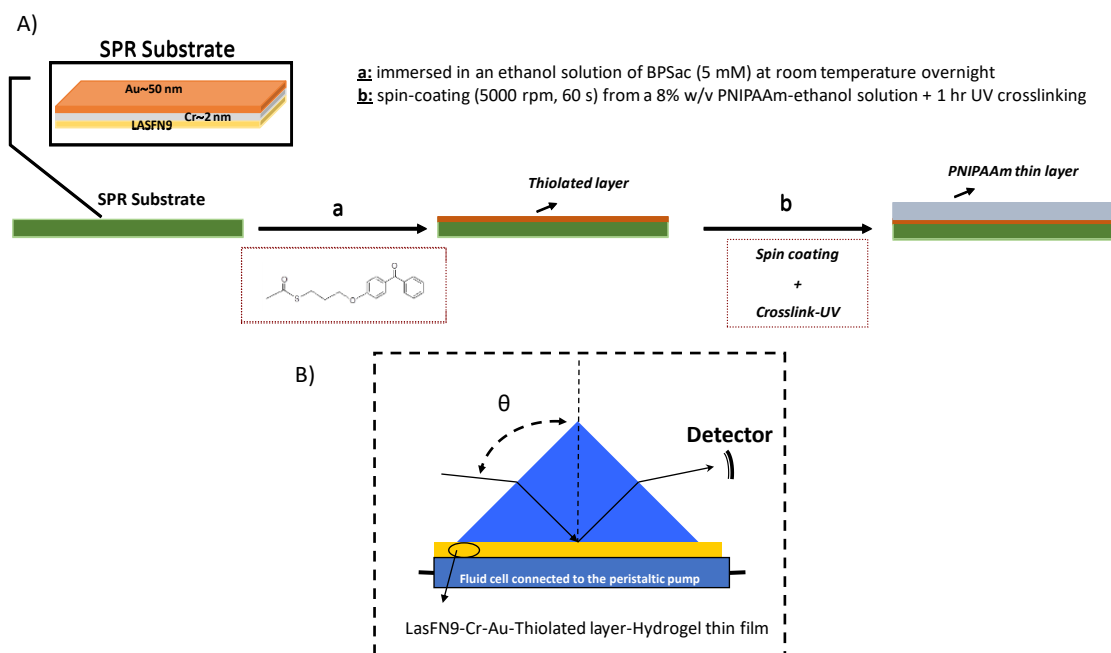


Figure 5. (a) Sample preparation for SPR measurements, (b) schematic representation of SPR sample holder with hydrogel layer and flow cell in Kretschmann configuration.

3.4. Surface plasmon resonance/optical waveguide spectroscopy (SPR/OWS) measurements

A custom-made setup in a Kretschmann configuration was used for SPR measurements as described in the literature as shown in Figure 5b [37–40]. LaSFN9 glass with a refractive index (n) of 1.8449 was used as a substrate and its uncoated side was matched to the base of a glass prism (LASFN9 prism). A He/Ne laser at $\lambda = 632.8$ nm (Uniphase) (monochromatic, linear, transverse magnetic (TM, p) polarization (Glan-Thompson polarizer, B, Hale)) was used as a light source and directed through the prism. A two-cycle goniometer (resolution of 0.05° , Huber) was used to change the external angle of incidence (θ), and angle-dependent intensities, $I(\theta)$, were recorded by collecting the light using a BPW 24 B silicon photodiode. Fresnel equations with transfer matrix algorithms [5] for a multilayer system were used to model the angle-dependent intensities using software called “Winspill” developed at the Max Plank Institute for Polymer Research, Mainz, Germany. Every layer in this model was defined by its thickness (d_{layer}) and complex dielectric constant, ϵ_{layer} ($\epsilon = \epsilon' + i\epsilon''$). The multilayer system consists of LASFN9 glass, chromium (d_{cr} , ϵ_{cr}), gold (d_{Au} , ϵ_{Au}), BPSAc (d_{BPSAc} , ϵ_{BPSAc}), hydrogel (d_{gel} , ϵ_{gel}), and salty water ($\epsilon_{water} = 1.77$). A reference scan was taken before the modification of the substrate using BPSAc in order to determine substrate parameters (d_{cr} , ϵ_{cr} , d_{Au} , ϵ_{Au}). A second scan ($I(\theta)$) was taken after modifying the substrate with BPSAc and d_{BPSAc} and ϵ_{BPSAc} to determine the BPSAc layer parameters assuming that all other parameters (d_{cr} , ϵ_{cr} , d_{Au} , ϵ_{Au}) are fixed. A third scan ($I(\theta)$) after spin coating and crosslinking the hydrogel layer was performed to obtain the parameter of the hydrogel layer (d_{gel} , ϵ_{gel}) in the dry state. OWS [22] can be performed with the same setup when the organic layer on the substrate is thicker than 500 nm. In that case, besides surface plasmon, optical waveguide modes can also be observed. These modes directly depend on the refractive index and the thickness of the organic layer (hydrogel layer in our case), and the layers can be characterized in detail. In order to analyze the

refractive index and the thickness of the hydrogel gel layers during collapse and swelling cycles from reflection scans, “a box model” that assumes an average refractive index for the whole layer was used. During swelling and collapse, the thickness and the refractive index of the hydrogel layers change at the same time. To calculate the thickness and the refractive index severally, hydrogels layers that have thicknesses higher than 500 nm were used to observe at least two optical modes. In order to see the optical waveguide modes, the thickness of hydrogel layers was chosen to be between 1 and 1.2 μm in the dry state for the measurements in the present study.

3.5. Swelling experiments

The salt-induced swelling behavior of PNIPAAm terpolymer thin layers was examined at room temperature using three different salt solutions (NAI, NaClO_4 , and Na_2CO_3) having concentrations in the range of 10^{-7} – 1 M. The measurements were done via placing the sample (LaSFN9-Cr-Au-BPSac-PNIPAAm terpolymer) onto a flow cell that was connected to a peristaltic pump (Figure 5b). Before starting the swelling experiments in salt solutions, the angle scan ($I(\theta)$) of the PNIPAAm terpolymer layer in the dry state was taken and then the flow cell was filled with distilled water. The layer was left to swell for 30 min and another angle scan ($I(\theta)$) was done. Then salt solution was injected into the flow using a peristaltic pump starting from the lowest concentration, the gel layer was again left to equilibrate for 30 min, and another angle scan was taken. The salt solution was changed to the following higher concentration and measurement was done in the same way. The process was repeated for all salt concentrations.

Acknowledgment

This research is supported by Gebze Technical University Research Fund (Project Number: GTU 2013-A30).

References

1. Hirokawa Y, Tanaka T. Volume phase transition in a nonionic gel. *The Journal of Chemical Physics* 1984; 81: 6379-6380. doi: 10.1063/1.447548
2. Junk MJN, Jonas U, Hinderberger D. EPR spectroscopy reveals nanoinhomogeneities in the structure and reactivity of thermoresponsive hydrogels. *Small* 2008; 4 (9): 1485-1493. doi: 10.1002/sml.200800127
3. Tanaka T, Fillmore D, Sun ST, Nishio I, Swislow G et al. Phase transitions in ionic gels. *Physical Review Letters* 1980; 45: 1636-1639. doi: 10.1103/PhysRevLett.45.1636
4. Eichenbaum GM, Kiser PF, Simon SA, Needham D. pH and ion-triggered volume response of anionic hydrogel microspheres. *Macromolecules* 1998; 31 (15): 5084-5093. doi: 10.1021/ma970897t
5. Krasovitski E, Cohen Y, Bianco-Peled HJ. The effect of salts on the conformation and microstructure of poly(N-isopropylacrylamide) (PNIPA) in aqueous solution. *Journal of Polymer Science: Part B Polymer Physics* 2004; 42 (20): 3713-3720. doi:10.1002/polb.20221
6. Harmon ME, Jakob TAM, Knoll W, Frank CW. A surface plasmon resonance study of volume phase transitions in n-isopropylacrylamide gel films. *Macromolecules* 2002; 35 (15): 5999-6004. doi: 10.1021/ma010985k
7. Kato N, Yamanobe S, Takahashi F. Property of magneto-driven poly (N-isopropylacrylamide) gel containing $\gamma\text{-Fe}_2\text{O}_3$ in NaCl solution as a chemomechanical device. *Materials Science and Engineering: C Materials for Biological Applications* 1997; 5 (2): 141-147. doi: 10.1016/S0928-4931(97)00030-1
8. Tanaka T, Nishio I, Sun ST, Ueno-Nishio S. Collapse of gels in an electric field. *Science* 1982; 218 (4571): 467-469. doi: 10.1126/science.218.4571.467

9. Schmaljohann D. Thermo- and pH-responsive polymers in drug delivery. *Advanced Drug Delivery Reviews* 2006; 58 (15), 1655-1670. doi: 10.1016/j.addr.2006.09.020
10. Lewis G, Coughlan DC, Lane ME, Corrigan OI. Preparation and release of model drugs from thermally sensitive poly(*N*-isopropylacrylamide) based microspheres. *Journal of Microencapsulation* 2006; 23 (6): 677-685. doi:10.1080/02652040600789237
11. Reber N, Spohr R, Wolf A, Omichi H, Tamada M et al. Closure characteristics of a thermally responsive single ion-track pore determined by size exclusion method. *Journal of Membrane Science* 1998; 140 (2): 275-281. doi:10.1016/S0376-7388(97)00279-2
12. Liang L, Feng XD, Martin PFC, Peurrung LM. Temperature-sensitive switch from composite poly(*N*-isopropylacrylamide) sponge gels. *Journal of Applied Polymer Science* 2000; 75 (14): 1735-1739. doi:10.1002/(SICI)1097-4628(20000401)75:14<1735::AID-APP7>3.0.CO;2-R
13. Wang Y, Brunsen A, Jonas U, Dostalek J, Knoll W. Prostate specific antigen biosensor based on long range surface plasmon-enhanced fluorescence spectroscopy and dextran hydrogel binding matrix. *Analytical Chemistry* 2009; 81 (23): 9625-9632. doi: 10.1021/ac901662e.
14. Kanazawa H, Matsushima Y, Okano T. Temperature-responsive chromatography. In: Brown PR, Grushka E (editors). *Advances in Chromatography*. New York, NY, USA: CRC Press, 2001, volume 41, pp. 311-316.
15. Tokarev I, Minko S. Stimuli-responsive hydrogel thin films. *Soft Matter* 2009; 5: 511-524. doi: 10.1039/B813827C
16. Anac I, Aulasevich A, Junk MJN, Jakubowicz P, Roskamp RF et al. Optical characterization of co-nonsolvency effects in thin responsive PNIPAAm-based gel layers exposed to ethanol/water mixtures. *Macromolecular Chemistry and Physics* 2010; 211: 1018-1025. doi: 10.1002/macp.200900533
17. Junk MJ N, Anac I, Menges B, Jonas U. Analysis of optical gradient profiles during temperature- and salt-dependent swelling of thin responsive hydrogel films. *Langmuir* 2010; 26 (14): 12253-12259. doi: 10.1021/la101185q
18. Harmon ME, Kuckling D, Frank CW. Photo-cross-linkable PNIPAAm copolymers. 2. Effects of constraint on temperature and pH-responsive hydrogel layers. *Macromolecules* 2003; 36 (1): 162-172. doi: 10.1021/ma021025g
19. Harmon ME, Kuckling D, Pareek P, Frank CW. Photo-cross-linkable PNIPAAm copolymers. 4. Effects of copolymerization and cross-linking on the volume-phase transition in constrained hydrogel layers. *Langmuir* 2003; 19 (26): 10947-10956. doi: 10.1021/la030217h
20. Toomey RG, Freidank D, Ruhe J. Swelling behavior of thin, surface-attached polymer networks. *Macromolecules* 2004; 37 (3): 882-887. doi: 10.1021/ma034737v
21. Schmidt S, Motschmann H, Hellweg T, von Klitzing R. Thermoresponsive surfaces by spin-coating of PNIPAM-co-PAA microgels: a combined AFM and ellipsometry study. *Polymer* 2008; 49 (4): 749-756. doi: 10.1016/j.polymer.2007.12.025
22. Beines PW, Klosterkamp I, Menges B, Jonas U, Knoll W. Responsive thin hydrogel layers from photo-cross-linkable poly(*N*-isopropylacrylamide) terpolymers. *Langmuir* 2007; 23 (4): 2231-2238. doi: 10.1021/la063264t
23. Vidyasagar A, Smith HL, Majewski J, Toomey RG. Continuous and discontinuous volume-phase transitions in surface-tethered, photo-crosslinked poly(*N*-isopropylacrylamide) networks. *Soft Matter* 2009; 5 (23), 4733-4738. doi: 10.1039/B904963K
24. van den Brom C, Anac I, Roskamp RF, Retsch M, Jonas U et al. The swelling behaviour of thermoresponsive hydrogel/silica nanoparticle composites. *Journal of Materials Chemistry* 2010; 20 (23): 4827-4839. doi: 10.1039/b927314j
25. Gianneli M, Beines PW, Roskamp RF, Koynov K, Fytas G et al. Local and global dynamics of transient polymer networks and swollen gels anchored on solid surfaces. *Journal of Physical Chemistry C* 2007; 111 (35): 13205-13211. doi: 10.1021/jp0728959

26. Raccis R, Roskamp R, Hopp I, Menges B, Koynov K et al. Probing mobility and structural inhomogeneities in grafted hydrogel films by fluorescence correlation spectroscopy. *Soft Matter* 2011; 7 (15): 7042-7053. doi: 10.1039/C0SM01438A
27. Gianneli M, Roskamp RF, Jonas U, Loppinet B, Fytas G et al. Dynamics of swollen gel layers anchored to solid surfaces. *Soft Matter* 2008; 4 (7): 1443-1447. doi: 10.1039/B801468J
28. Gianneli M, Anac I, Roskamp R, Menges B, Loppinet B et al. Dynamic response of anchored poly(*N*-isopropylacrylamide-co-methacrylic acid-co-benzophenone methacrylate) terpolymer hydrogel layers to physicochemical stimuli. *Macromolecular Chemistry and Physics* 2015; 216: 277-286. doi: 10.1002/macp.201400361
29. Ishida N, Biggs S. Salt-induced structural behavior for poly(*N*-isopropylacrylamide) grafted onto solid surface observed directly by AFM and QCM-D. *Macromolecules* 2007; 40 (25): 9045-9052. doi:10.1021/ma071878e
30. Naini CA, Thomas M, Franzka S, Frost S, Ulbricht M et al. Hofmeister effect of sodium halides on the switching energetics of thermoresponsive polymer brushes. *Macromolecular Rapid Communications* 2013; 34 (5): 417-422. doi:10.1002/marc.201200681
31. Murdoch TJ, Humphreys BA, Willott JD, Gregory KP, Prescott SW et al. Specific anion effects on the internal structure of a poly(*N*-isopropylacrylamide) brush. *Macromolecules* 2016; 49 (16): 6050-6060. doi: 10.1021/acs.macromol.6b01001
32. Humphreys BA, Willott JD, Murdoch TJ, Webber GB, Wanless EJ. Specific ion modulated thermoresponse of poly(*N*-isopropylacrylamide) brushes. *Physical Chemistry Chemical Physics* 2016; 18 (8): 6037-6046. doi: 10.1039/C5CP07468A
33. Koenig M, Rodenhausen KB, Rauch S, Bittrich E, Eichhorn KJ et al. Salt sensitivity of the thermoresponsive behavior of PNIPAAm brushes. *Langmuir* 2018; 34 (7): 2448-2454. doi: 10.1021/acs.langmuir.7b039
34. Schild HG. Poly(*N*-isopropylacrylamide): experiment, theory and application. *Progress in Polymer Science* 1992; 17 (2): 163-249. doi:10.1016/0079-6700(92)90023
35. Prucker O, Naumann CA, Rhe J, Knoll W, Frank CW. Photochemical attachment of polymer films to solid surfaces via monolayers of benzophenone derivatives. *Journal of American Chemical Society* 1999; 121 (38): 8766-8770. doi: 10.1021/ja990962+
36. Biesalski M, Johannsmann D, Rhe J. Synthesis and swelling behavior of a weak polyacid brush. *The Journal of Chemical Physics* 2002; 117: 4988-4994. doi: 10.1063/1.1490924
37. Knoll W. Interfaces and thin films as seen by bound electromagnetic waves. *Annual Review of Physical Chemistry* 1998; 4: 569-638. doi: 10.1146/annurev.physchem.49.1.569
38. Born M, Wolf E. Principles of Optics: Electromagnetic Theory of Propagation, Interference and Diffraction of Light. Cambridge UK: Cambridge University Press, 1999.
39. Acikbas Y, Taktak F, Capan F, Tuncer C, Butun V et al. An optical vapor sensor based on amphiphilic block copolymer Langmuir–Blodgett films. *IEEE Sensors Journal* 2018; 18 (13): 5313-5320. doi:10.1109/JSEN.2018.2833491
40. Acikbas Y, Capan F, Erdogan M, Bulut L, Soykan C. Optical characterization and swelling behaviour of Langmuir–Blodgett thin films of a novelpoly[(Styrene (ST)-co-Glycidyl Methacrylate (GMA)]. *Sensor and Actuators B: Chemical* 2017; 241: 1111-1120. doi: 10.1016/j.snb.2016.10.025